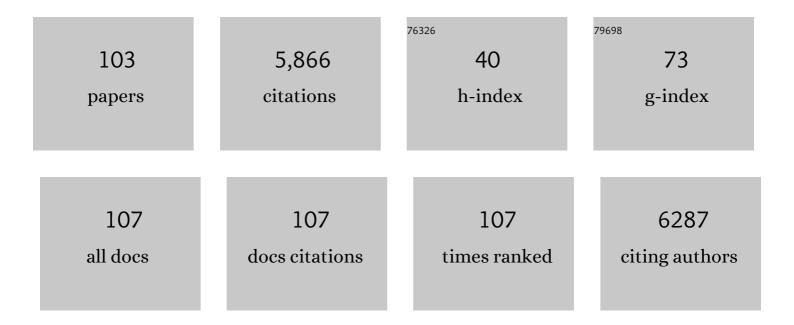
Marc E Levenston

List of Publications by Year in descending order

Source: https://exaly.com/author-pdf/4163826/publications.pdf Version: 2024-02-01



#	Article	IF	CITATIONS
1	Cartilage Tissue Remodeling in Response to Mechanical Forces. Annual Review of Biomedical Engineering, 2000, 2, 691-713.	12.3	548
2	Mechanical confinement regulates cartilage matrix formation by chondrocytes. Nature Materials, 2017, 16, 1243-1251.	27.5	348
3	Injurious Mechanical Compression of Bovine Articular Cartilage Induces Chondrocyte Apoptosis. Archives of Biochemistry and Biophysics, 2000, 381, 205-212.	3.0	311
4	Analysis of cartilage matrix fixed charge density and three-dimensional morphology via contrast-enhanced microcomputed tomography. Proceedings of the National Academy of Sciences of the United States of America, 2006, 103, 19255-19260.	7.1	264
5	Biomechanical analysis of silicon microelectrode-induced strain in the brain. Journal of Neural Engineering, 2005, 2, 81-89.	3.5	239
6	Inhibition of in vitro chondrogenesis in RGD-modified three-dimensional alginate gels. Biomaterials, 2007, 28, 1071-1083.	11.4	197
7	Dynamic Compression Regulates the Expression and Synthesis of Chondrocyte-Specific Matrix Molecules in Bone Marrow Stromal Cells. Stem Cells, 2007, 25, 655-663.	3.2	164
8	A versatile shear and compression apparatus for mechanical stimulation of tissue culture explants. Journal of Biomechanics, 2000, 33, 1523-1527.	2.1	162
9	Mechanical compression alters gene expression and extracellular matrix synthesis by chondrocytes cultured in collagen I gels. Biomaterials, 2002, 23, 1249-1259.	11.4	152
10	Chondrocyte phenotypes on different extracellular matrix monolayers. Biomaterials, 2004, 25, 5929-5938.	11.4	150
11	Numerical instabilities in bone remodeling simulations: The advantages of a node-based finite element approach. Journal of Biomechanics, 1995, 28, 449-459.	2.1	147
12	Dynamic compression of chondrocyte-seeded fibrin gels: effects on matrix accumulation and mechanical stiffness. Osteoarthritis and Cartilage, 2004, 12, 117-130.	1.3	136
13	Variations in matrix composition and GAG fine structure among scaffolds for cartilage tissue engineering. Osteoarthritis and Cartilage, 2005, 13, 828-836.	1.3	136
14	Bite-force estimation for Tyrannosaurus rex from tooth-marked bones. Nature, 1996, 382, 706-708.	27.8	132
15	Depth-Dependent Transverse Shear Properties of the Human Corneal Stroma. , 2012, 53, 873.		124
16	Quantitative assessment of articular cartilage morphology via EPIC-μCT. Osteoarthritis and Cartilage, 2009, 17, 313-320.	1.3	123
17	Self-assembling nanoparticles for intra-articular delivery of anti-inflammatory proteins. Biomaterials, 2012, 33, 7665-7675.	11.4	113
18	Interactions between integrin ligand density and cytoskeletal integrity regulate BMSC chondrogenesis. Journal of Cellular Physiology, 2008, 217, 145-154.	4.1	91

#	Article	IF	CITATIONS
19	Combined effects of growth factors and static mechanical compression on meniscus explant biosynthesis. Osteoarthritis and Cartilage, 2004, 12, 736-744.	1.3	88
20	Computer simulations of stress-related bone remodeling around noncemented acetabular components. Journal of Arthroplasty, 1993, 8, 595-605.	3.1	85
21	Nondestructive assessment of sGAG content and distribution in normal and degraded rat articular cartilage via EPIC-μCT. Osteoarthritis and Cartilage, 2010, 18, 65-72.	1.3	85
22	Numerical Approximation of Tangent Moduli for Finite Element Implementations of Nonlinear Hyperelastic Material Models. Journal of Biomechanical Engineering, 2008, 130, 061003.	1.3	84
23	Fact versus artifact: Avoiding erroneous estimates of sulfated glycosaminoglycan content using the dimethylmethylene blue colorimetric assay for tissue-engineered constructs. , 2015, 29, 224-236.		84
24	Cyclic Tensile Culture Promotes Fibroblastic Differentiation of Marrow Stromal Cells Encapsulated in Poly(Ethylene Glycol)-Based Hydrogels. Tissue Engineering - Part A, 2010, 16, 3457-3466.	3.1	75
25	3D imaging of tissue integration with porous biomaterials. Biomaterials, 2008, 29, 3757-3761.	11.4	74
26	Indentation testing of human articular cartilage: Effects of probe tip geometry and indentation depth on intra-tissue strain. Journal of Biomechanics, 2006, 39, 1039-1047.	2.1	70
27	Maturation and Integration of Tissue-Engineered Cartilages within an in Vitro Defect Repair Model. Tissue Engineering, 2004, 10, 736-746.	4.6	69
28	Meniscus and cartilage exhibit distinct intra-tissue strain distributions under unconfined compression. Osteoarthritis and Cartilage, 2010, 18, 1291-1299.	1.3	64
29	Improved method for analysis of whole bone torsion tests. Journal of Bone and Mineral Research, 1994, 9, 1459-1465.	2.8	62
30	Variations in chondrogenesis of human bone marrow-derived mesenchymal stem cells in fibrin/alginate blended hydrogels. Acta Biomaterialia, 2012, 8, 3754-3764.	8.3	61
31	Articular chondrocytes derived from distinct tissue zones differentially respond to in vitro oscillatory tensile loading. Osteoarthritis and Cartilage, 2008, 16, 1228-1236.	1.3	59
32	Variationally derived 3-field finite element formulations for quasistatic poroelastic analysis of hydrated biological tissues. Computer Methods in Applied Mechanics and Engineering, 1998, 156, 231-246.	6.6	58
33	Characterization of proteoglycan production and processing by chondrocytes and BMSCs in tissue engineered constructs. Osteoarthritis and Cartilage, 2008, 16, 1092-1100.	1.3	57
34	Ion-channel Regulation of Chondrocyte Matrix Synthesis in 3D Culture Under Static and Dynamic Compression. Biomechanics and Modeling in Mechanobiology, 2007, 6, 33-41.	2.8	56
35	Alterations in Physical Cross-Linking Modulate Mechanical Properties of Two-Phase Protein Polymer Networks. Biomacromolecules, 2005, 6, 3037-3044.	5.4	55
36	Quantitative imaging of cartilage and bone morphology, reactive oxygen species, and vascularization in a rodent model of osteoarthritis. Arthritis and Rheumatism, 2012, 64, 1899-1908.	6.7	55

#	Article	IF	CITATIONS
37	Mechanical properties of the airway tree: heterogeneous and anisotropic pseudoelastic and viscoelastic tissue responses. Journal of Applied Physiology, 2018, 125, 878-888.	2.5	53
38	Oscillatory tension differentially modulates matrix metabolism and cytoskeletal organization in chondrocytes and fibrochondrocytes. Journal of Biomechanics, 2004, 37, 1941-1952.	2.1	52
39	Regional variation in T1ϕand T2 times in osteoarthritic human menisci: correlation with mechanical properties and matrix composition. Osteoarthritis and Cartilage, 2013, 21, 796-805.	1.3	52
40	Tensile Loading Modulates Bone Marrow Stromal Cell Differentiation and the Development of Engineered Fibrocartilage Constructs. Tissue Engineering - Part A, 2010, 16, 1913-1923.	3.1	51
41	Central and peripheral region tibial plateau chondrocytes respond differently to in vitro dynamic compression. Osteoarthritis and Cartilage, 2009, 17, 980-987.	1.3	46
42	Regional variations in the distribution and colocalization of extracellular matrix proteins in the juvenile bovine meniscus. Journal of Anatomy, 2012, 221, 174-186.	1.5	46
43	Comparison of osmotic swelling influences on meniscal fibrocartilage and articular cartilage tissue mechanics in compression and shear. Journal of Orthopaedic Research, 2012, 30, 95-102.	2.3	43
44	Chondrocytes and Meniscal Fibrochondrocytes Differentially Process Aggrecan During <i>De Novo</i> Extracellular Matrix Assembly. Tissue Engineering - Part A, 2009, 15, 1513-1522.	3.1	40
45	Response of cartilage and meniscus tissue explants to inÂvitro compressive overload. Osteoarthritis and Cartilage, 2012, 20, 422-429.	1.3	37
46	An energy dissipation-based model for damage stimulated bone adaptation. Journal of Biomechanics, 1998, 31, 579-586.	2.1	32
47	Selective and non-selective metalloproteinase inhibitors reduce IL-1-induced cartilage degradation and loss of mechanical properties. Matrix Biology, 2007, 26, 259-268.	3.6	31
48	The influence of cyclic tension amplitude on chondrocyte matrix synthesis: experimental and finite element analyses. Biorheology, 2004, 41, 377-87.	0.4	31
49	Aggrecanolysis and in vitro matrix degradation in the immature bovine meniscus: mechanisms and functional implications. Arthritis Research and Therapy, 2009, 11, R173.	3.5	29
50	The role of loading memory in bone adaptation simulations. Bone, 1994, 15, 177-186.	2.9	27
51	Electrokinetic and Poroelastic Coupling During Finite Deformations of Charged Porous Media. Journal of Applied Mechanics, Transactions ASME, 1999, 66, 323-334.	2.2	27
52	Modulation of Mesenchymal Stem Cell Shape in Enzyme-Sensitive Hydrogels Is Decoupled from Upregulation of Fibroblast Markers Under Cyclic Tension. Tissue Engineering - Part A, 2012, 18, 2365-2375.	3.1	25
53	Different loads can produce similar bone density distributions. Bone, 1996, 19, 127-135.	2.9	24
54	Composition-function relationships during IL-1-induced cartilage degradation and recovery. Osteoarthritis and Cartilage, 2009, 17, 1029-1039.	1.3	24

#	Article	IF	CITATIONS
55	Observations of convergence and uniqueness of node-based bone remodeling simulations. Annals of Biomedical Engineering, 1997, 25, 261-268.	2.5	21
56	Meniscus is more susceptible than cartilage to catabolic and anti-anabolic effects of adipokines. Osteoarthritis and Cartilage, 2015, 23, 1551-1562.	1.3	21
57	Discrimination of meniscal cell phenotypes using gene expression profiles. , 2012, 23, 195-208.		19
58	Mechanisms of osteoarthritis in the knee: MR imaging appearance. Journal of Magnetic Resonance Imaging, 2014, 39, 1346-1356.	3.4	18
59	A variational formulation for coupled physicochemical flows during finite deformations of charged porous media. International Journal of Solids and Structures, 1998, 35, 4999-5019.	2.7	17
60	Loading Mode Interactions in Simulations of Long Bone Cross-Sectional Adaptation. Computer Methods in Biomechanics and Biomedical Engineering, 1998, 1, 303-319.	1.6	17
61	A constitutive model for protein-based materials. Biomaterials, 2006, 27, 5315-5325.	11.4	17
62	Bone Load Estimation for the Proximal Femur Using Single Energy Quantitative CT Data. Computer Methods in Biomechanics and Biomedical Engineering, 1998, 1, 233-245.	1.6	16
63	Comparison of Different Approaches for Measuring Tibial Cartilage Thickness. Journal of Integrative Bioinformatics, 2017, 14, .	1.5	15
64	Improved Estimation of Solute Diffusivity Through Numerical Analysis of FRAP Experiments. Cellular and Molecular Bioengineering, 2009, 2, 104-117.	2.1	14
65	Application of Advanced Magnetic Resonance Imaging Techniques in Evaluation of the Lower Extremity. Radiologic Clinics of North America, 2013, 51, 529-545.	1.8	14
66	Photochemical approaches for bonding of cartilage tissues. Osteoarthritis and Cartilage, 2009, 17, 1649-1656.	1.3	13
67	Osmotic Swelling Responses Are Conserved Across Cartilaginous Tissues With Varied Sulfatedâ€Glycosaminoglycan Contents. Journal of Orthopaedic Research, 2020, 38, 785-792.	2.3	13
68	Proximal Femoral Density Patterns are Consistent with Bicentric Joint Loads. Computer Methods in Biomechanics and Biomedical Engineering, 1999, 2, 271-283.	1.6	12
69	Range Imaging for Motion Compensation in C-Arm Cone-Beam CT of Knees under Weight-Bearing Conditions. Journal of Imaging, 2018, 4, 13.	3.0	12
70	Enhancing integration of articular cartilage grafts via photochemical bonding. Journal of Orthopaedic Research, 2018, 36, 2406-2415.	2.3	11
71	Detecting Anatomical Landmarks for Motion Estimation in Weight-Bearing Imaging of Knees. Lecture Notes in Computer Science, 2018, , 83-90.	1.3	11
72	Periosteal bone formation stimulated by externally induced bending strains. Journal of Bone and Mineral Research, 1995, 10, 671-671.	2.8	10

#	Article	IF	CITATIONS
73	Quantitative tracking of passage and 3D culture effects on chondrocyte and fibrochondrocyte gene expression. Journal of Tissue Engineering and Regenerative Medicine, 2017, 11, 1185-1194.	2.7	10
74	Co-culture with infrapatellar fat pad differentially stimulates proteoglycan synthesis and accumulation in cartilage and meniscus tissues. Connective Tissue Research, 2017, 58, 447-455.	2.3	10
75	On the impact of vessel wall stiffness on quantitative flow dynamics in a synthetic model of the thoracic aorta. Scientific Reports, 2021, 11, 6703.	3.3	10
76	Temporal stability of node-based internal bone adaptation simulations. Journal of Biomechanics, 1997, 30, 403-407.	2.1	9
77	Bovine meniscal tissue exhibits age- and interleukin-1 dose-dependent degradation patterns and composition-function relationships. Journal of Orthopaedic Research, 2016, 34, 801-811.	2.3	9
78	Rapid volumetric gagCEST imaging of knee articular cartilage at 3 T: evaluation of improved dynamic range and an osteoarthritic population. NMR in Biomedicine, 2020, 33, e4310.	2.8	9
79	A modified lap test to more accurately estimate interfacial shear strength for bonded tissues. Journal of Biomechanics, 2008, 41, 3260-3264.	2.1	8
80	Characterizing the transient response of knee cartilage to running: Decreases in cartilage <i>T</i> ₂ of female recreational runners. Journal of Orthopaedic Research, 2021, 39, 2340-2352.	2.3	8
81	Adipokines induce catabolism of newly synthesized matrix in cartilage and meniscus tissues. Connective Tissue Research, 2017, 58, 246-258.	2.3	7
82	Epipolar Consistency Conditions for Motion Correction in Weight-Bearing Imaging. Informatik Aktuell, 2017, , 209-214.	0.6	6
83	Tibial cartilage creep during weight bearing: in vivo 3D CT assessment. Osteoarthritis and Cartilage, 2016, 24, S104.	1.3	4
84	Validation of watershed-based segmentation of the cartilage surface from sequential CT arthrography scans. Quantitative Imaging in Medicine and Surgery, 2021, 12, 0-0.	2.0	4
85	JOINT calibration and motion estimation in weight-bearing cone-beam CT of the knee joint using fiducial markers. , 2017, , .		3
86	Evaluating the relationship between gagCEST MRI and cartilage biochemical composition in juvenile bovine articular cartilage. Osteoarthritis and Cartilage, 2019, 27, S369.	1.3	3
87	Development and Finite Element Implementation of a Nearly Incompressible Structural Constitutive Model for Artery Substitute Design. , 2008, , .		2
88	Over-exposure correction in knee cone-beam CT imaging with automatic exposure control using a partial low dose scan. , 2016, , .		2
89	Feasibility of Motion Compensation using Inertial Measurement in C-arm CT. , 2018, , .		2
90	Rapid and durable photochemical bonding of cartilage using the porphyrin photosensitizer verteporfin. Osteoarthritis and Cartilage, 2019, 27, 1537-1544.	1.3	2

#	Article	IF	CITATIONS
91	Automatic Orientation Estimation of Inertial Sensors in C-Arm CT Projections. Current Directions in Biomedical Engineering, 2019, 5, 195-198.	0.4	2
92	Motion Compensation Using Range Imaging in C-Arm Cone-Beam CT. Communications in Computer and Information Science, 2017, , 561-570.	0.5	2
93	Contrast-Enhanced Micro-CT Imaging of Soft Tissues. , 2007, , 239-256.		1
94	Chondrocytes and Fibrochondrocytes Differentially Process Aggrecan During De Novo Extracellular Matrix Assembly. , 2007, , 1041.		0
95	Osmotic Effects on the Dynamic Shear Properties of Meniscal Fibrocartilage. , 2008, , .		Ο
96	Are Passaged Chondrocytes Phenotypically Similar to Meniscal Fibrochondrocytes?. , 2010, , .		0
97	Object removal in gradient domain of cone-beam CT projections. , 2016, , .		Ο
98	Depth Dependent Diffusivity Profile in Bovine Articular Cartilage: Comparing Transverse and Axial Diffusivities. , 2007, , .		0
99	Articular Cartilage and Meniscal Fibrocartilage Mechanics: Evidence for Differences in Ultrastructure and Function of Proteoglycans. , 2009, , .		Ο
100	Outside-In vs. Inside-Out: Contrasting Patterns of Compressive Deformation in Cartilage and Meniscus. , 2010, , .		0
101	Dose-Dependent Effects of Interleukin-1Alpha on Functional Degradation of Lateral and Medial Menisci. , 2010, , .		Ο
102	Self-Calibration and Simultaneous Motion Estimation for C-Arm CT Using Fiducial. Informatik Aktuell, 2017, , 56-61.	0.6	0
103	Smooth Ride: Low-Pass Filtering of Manual Segmentations Improves Consensus. Informatik Aktuell, 2019, , 86-91.	0.6	0